HHS Public Access

Author manuscript

Mol Microbiol. Author manuscript; available in PMC 2018 January 01.

Published in final edited form as:

Mol Microbiol. 2017 January ; 103(2): 214–228. doi:10.1111/mmi.13551.

Bordetella Adenylate Cyclase Toxin Interacts with Filamentous Haemagglutinin to Inhibit Biofilm Formation *in vitro*

Casandra Hoffman[1], **Joshua Eby**[1], **Mary Gray**[1], **F. Heath Damron**[2], **Jeffrey Melvin**[3], **Peggy Cotter**[3], and **Erik Hewlett**[1,a]

[1]Division of Infectious Diseases and International Health, Department of Medicine, University of Virginia, Charlottesville, VA

[2]Department of Microbiology, Immunology and Cell Biology, School of Medicine, West Virginia University, Morgantown, WV

[3]School of Medicine, University of North Carolina, Chapel Hill, NC

[a]To whom correspondence should be addressed: Erik L. Hewlett, M.D., Division of Infectious Diseases and International Health, Department of Medicine, University of Virginia, 345 Crispell Drive, RM 1706, Charlottesville, VA 22908, Tel: 434-924-4334, EH2V@hscmail.mcc.virginia.edu.

All authors have no conflict of interest.

SUPPLEMENTARY FIGURE LEGENDS

Figure S1. Growth curves of bacterial strains grown in SSM **(A)** shaking 10 mL culture **(B)** static 100μL culture in 96 well plates. OD_{600} measurements recorded over 24 hours for shaking cultures and 96 hours for static 100 μL cultures.

Figure S2. (A) *B. pertussis* strains were grown in 5 mL cultures and increasing concentrations of urea were added to ensure urea had no effect on bacterial growth. Data expressed as the mean ± standard deviations, compiled from 3 experiments run in triplicate. **(B)** Static 100μL cultures were grown in the presence and absence of ACT or AC domain in 96 well plates. OD_{600} measurements were recorded every 24 hours.

Figure S3. (A) ACT inhibits *B. bronchiseptica* biofilm in a concentration-dependent manner. WT RB50 biofilm formation in the presence of increasing concentrations of recombinant purified ACT (10, 100, or 1000 ng mL^{-1}) for 96 hours. Biofilm formation was measured by crystal violet assay. Bvg(−) RB54 strain serves as negative control. Data expressed as the mean ± standard deviations, compiled from 3 experiments run in triplicate. ** = p <0.01 and *** = p <0.001 compared to WT without ACT. **(B) The AC domain is necessary and sufficient for *B. bronchiseptica* biofilm inhibition, although the catalytic activity of ACT is not required**. ACT, iACT or other ACT truncated mutant proteins were added to RB50 and biofilm formation was measured by crystal violet assay at 96 hours. AC domain was added at 10 ng mL^{-1} and additional ACT proteins including ΔH, ΔHR1, ΔR, and ΔAC were all added to a final concentration of 100 ng mL^{-1}. Bvg(−) RB54 strain serves as negative control. Data expressed as the mean ± standard deviations, compiled from 3 experiments run in triplicate. ** = p <0.01 compared to WT RB50

Figure S4. AC domain inhibits biofilm in a concentration-dependent manner. BP338 biofilm formation in the presence of increasing concentrations of recombinant purified ACT (10, 100, or 1000 ng mL^{-1}) for 96 hours. Biofilm formation was measured by crystal violet assay. Bvg(-) strain serves as negative control. Data expressed as the mean ± standard deviations, compiled from 3 experiments run in triplicate. * = p <0.05, ** = p <0.01, *** = p <0.001, **** = p <0.0001 compared to WT without ACT.

Figure S5. Western blot of BP338 ΔAC, confirmation of deletion of AC domain. Bacterial strains were grown 48 hours on BG plates at 37ºC, transferred to 10 mL shaking SSM cultures, and grown for 24 hours. At 24 hours samples were taken and the OD_{600} of each sample was matched. Samples were boiled 5 minutes and 30 μL of the sample was loaded per well. 1 μg of ACT was loaded. A western blot was performed using a polyclonal ACT antibody (Lee *et al*, 1995).

Figure S6. Purified proteins used in SPR experiments. 10 μg of each protein was loaded into wells of a 7.5% SDS-PAGE gel. Coomassie staining shows purity of proteins used in SPR experiments.

Figure S7. (A) Biofilm time course of WT *B. pertussis* strains used in the study, BP338 and BPSM **(B)** ACT and FHA protein expression of BP338 and BPSM at 24 hours in shaking culture. 20 μL of OD_{600} normalized bacteria were run on SDS-PAGE gel and protein expression was determined by western blot analysis; polyclonal anti-ACT antibody was used to detect ACT and monoclonal anti-CRD antibody (Noel *et al*., 2012) was used to detect FHA.

Figure S8. The MCD of FHA must be present and properly folded for ACT inhibition of *B. bronchiseptica* biofilm. FHA mutant proteins were generated in the WT *B. bronchiseptica* RBX11 parent strain. JS20 (ΔMCD) has the entire MCD sequence deleted. RBX11 T-N has a transposon inserted into the prodomain sequence, precluding prodomain cleavage and processing of the MCD, leaving the MCD unfolded in the final FHA molecule. *B. bronchiseptica* strains were allowed to form biofilm for 96 hours in the presence or absence of ACT. Biofilm was measured by crystal violet assay. Data expressed as the mean ± standard deviations, compiled from 3 experiments run in triplicate.** = p <0.01 and *** = p<0.001 compared to WT (RB50).

SUMMARY

Bordetella pertussis, the causative agent of whooping cough, secretes and releases adenylate cyclase toxin (ACT), which is a protein bacterial toxin that targets host cells and disarms immune defenses. ACT binds filamentous hemagglutinin (FHA), a surface-displayed adhesin, and until now, the consequences of this interaction were unknown. A *B. bronchiseptica* mutant lacking ACT produced more biofilm than the parental strain; leading Irie *et al.* to propose the ACT-FHA interaction could be responsible for biofilm inhibition. Here we characterize the physical interaction of ACT with FHA and provide evidence linking that interaction to inhibition of biofilm *in vitro*. Exogenous ACT inhibits biofilm formation in a concentration-dependent manner and the N-terminal catalytic domain of ACT (AC domain) is necessary and sufficient for this inhibitory effect. AC Domain interacts with the C-terminal segment of FHA with ~650 nM affinity. ACT does not inhibit biofilm formation by *Bordetella* lacking the mature C-terminal domain (MCD), suggesting the direct interaction between AC domain and the MCD is required for the inhibitory effect. Additionally, AC domain disrupts preformed biofilm on abiotic surfaces. The demonstrated inhibition of biofilm formation by a host-directed protein bacterial toxin represents a novel regulatory mechanism and identifies an unprecedented role for ACT.

Graphical Abstract

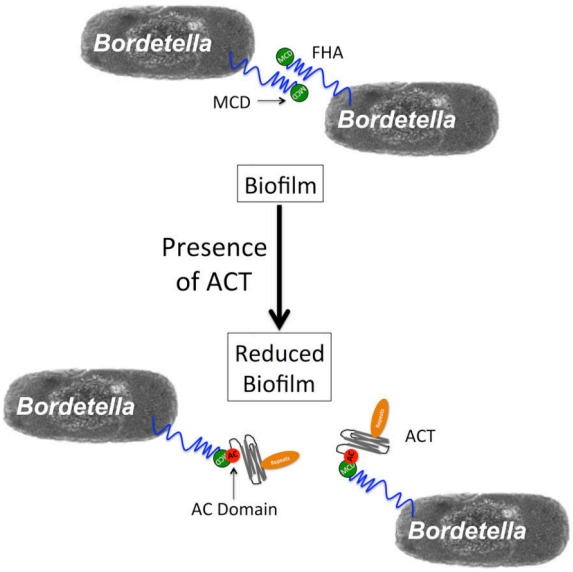

ABBREVIATED SUMMARY

The catalytic domain (AC domain) of *Bordetella* Adenylate Cyclase Toxin (ACT) interacts with the distal tip of Filamentous Hemagglutinin, the mature C-terminal domain with approximately 650 nM affinity. This interaction results in the inhibition of biofilm formation by *B. pertussis* and *B. bronchiseptica in vitro*. Despite the AC domain being necessary and sufficient for inhibition, the catalytic activity of ACT is not required for biofilm inhibition.

INTRODUCTION

Bordetella pertussis is the causative agent of whooping cough (pertussis) and a reemerging health threat in the United States and globally, as illustrated by the increasing number of cases reported each year. Despite high vaccination rates of children and adolescents, there were approximately 33,000 cases in the United States reported to the CDC in 2014. The most striking shift in the age-specific incidence of pertussis has been in patients aged 15 and older (Strebel *et al.*, 2001), who are now more frequently infected with *B. pertussis*. In contrast to the potential fatality of pertussis in infants and young children, adolescents and adults develop a persistent cough with fewer systemic manifestations of the disease (Birkebaek *et al.*, 1999; Wendelboe *et al.*, 2007) and often serve as sources of pertussis transmission (Nelson, 1978; Cherry and Olin, 1999; Bisgard *et al.*, 2004; Quinn and McIntyre, 2011).

B. pertussis has been shown to form biofilm *in vitro* on abiotic surfaces and *in vivo*, primarily on nasal septum and the trachea (Sloan *et al.*, 2007; Serra *et al.*, 2007; Conover *et al.*, 2010; Serra *et al.*, 2011). Ongoing studies support the concept that *B. pertussis* forms biofilm during infection; recent clinical isolates form more biofilm compared to a lab-passaged isolate, BP338, and de Gouw *et al.* showed that biofilm-derived antigens protect mice from *B. pertussis* infection (de Gouw *et al.*, 2014; Arnal *et al.*, 2015). The closely related animal pathogen, *B. bronchiseptica* forms biofilm *in vitro* on abiotic surfaces and biofilm formation contributes to its chronic infection of dogs and other mammals (Fenwick, 2013). Although the specific role of biofilm in human infections with *B. pertussis* has not yet been established, it is clear that these organisms produce biofilm both *in vitro* and *in vivo* and thus the regulation of this process warrants further investigation.

Biofilms are complex structures controlled by a variety of bacterial signaling systems. They are comprised of aggregative bacteria surrounded by a matrix of polysaccharides, proteins and extracellular DNA (eDNA). *Bordetella* biofilm has been shown to require eDNA (Conover *et al.*, 2011), Bps (*Bordetella* polysaccharide) (Conover *et al.*, 2010), which resembles *S. aureus* poly-N-acetyl-beta-(1–6)-glucosamine, and multiple proteins. Of significance to this study is the observation that filamentous hemagglutinin (FHA) is an important component of *B. pertussis* and *B. bronchiseptica* biofilm formation. This surface displayed adhesin promotes the formation and maintenance of biofilm by mediating bacteria-substrate as well as bacteria-bacteria interactions. Serra *et al.* showed that anti-FHA antibodies blocked biofilm formation by *B. pertussis*, and a strain lacking FHA (Δ*fhaB* BPGR4) made less biofilm *in vitro* and *in vivo* on mouse trachea and nasal septum compared to WT BPSM (Serra *et al.*, 2011).

Although less is known about the regulation of biofilm in *Bordetellae* compared to other medically relevant biofilm-forming bacterial species, several modes of regulation have been implicated. Nutrient limitation and oxidative stress activate (p)ppGpp signaling to enhance biofilm formation in *B. pertussis* (Sugisaki *et al.*, 2013), while c-di-GMP signaling regulates motility and biofilm formation in *B. bronchiseptica* (Sisti *et al.*, 2013). The machinery for synthesis of the Bps matrix component is encoded by the *bpsABCD* operon and is under control of the BpsR repressor, but the factor, process, or signal that relieves BpsR repression

is unknown (Conover *et al.*, 2012). Multiple signals, including those from the "master regulator" of virulence, *Bordetella* virulence gene two-component regulatory system, BvgAS, are integrated to control *Bordetella* biofilm. Biofilm formation occurs in the Bvg(+) phase and Bvg(i) phase, but biofilm is not observed in the Bvg(−) phase. Irie *et al.* showed biofilm formation was maximal in the Bvg(i) phase in *B. bronchiseptica* (Irie *et al.*, 2004). In contrast, Mishra *et al.* found biofilm formation was equal in the Bvg(+) and Bvg(i) phases for *B. pertussis* (Mishra *et al.*, 2005). Irie *et al.* also showed that a *B. bronchiseptica* strain lacking adenylate cyclase toxin (ACT) (Δ*cyaA* RB58) made more biofilm than the parental WT RB50 strain and in light of the earlier observation demonstrating a direct interaction between ACT and FHA (Zaretzky *et al.*, 2002), suggested that this protein-protein interaction could function to regulate biofilm production in *Bordetella*.

ACT is an important virulence factor of both *B. pertussis* and *B. bronchiseptica*. The 177 kDa protein toxin is secreted by a type I secretion system and remains surface-associated or is released as a function of free calcium concentration in the medium (Bumba *et al.*, 2016). ACT that has been released from the bacterial surface is the active form of the toxin, which affects target cells (Gray *et al.*, 2004). ACT uses complement receptor 3, the heterodimeric $\alpha_M\beta_2$ integrin (CD11b/CD18 or Mac-1), as its receptor (Guermonprez *et al.*, 2001; Osicka *et al.*, 2015), but can also intoxicate cells that lack this integrin heterodimer (Eby *et al.*, 2010). Following binding to the host cell, the catalytic domain of the toxin is translocated across the plasma membrane and into the host cytoplasm, where calmodulin (CaM) binds the enzymatic (catalytic) domain, activating it to convert ATP → cAMP (Guermonprez *et al.*, 2001; El-Azami-El-Idrissi *et al.*, 2003; Perkins *et al.*, 2007; Martin *et al.*, 2010; Osickova *et al.*, 2010; Eby *et al.*, 2012; Uribe *et al.*, 2013). This in turn leads to supraphysiological levels of cAMP and can cause a massive reduction in intracellular ATP (Basler *et al.*, 2006; Hewlett *et al.*, 2006; Bumba *et al.*, 2010; Eby *et al.*, 2012). Through these mechanisms, ACT inhibits phagocytosis, chemotaxis, and superoxide generation by neutrophils, is required for the establishment of infection in the mouse model and human infections with the attenuated strain, BPZE1 (Thorstensson *et al.*, 2014; Lim *et al.*, 2014) and serves as a protective antigen (Confer and Eaton, 1982; Weiss *et al.*, 1983; Pearson *et al.*, 1987; Cherry and Heinninger, 2004; Vojtova *et al.*, 2006; Basler *et al.*, 2006; Hewlett *et al.*, 2006; Fiser *et al.*, 2012; Costache *et al.*, 2013; Fedele *et al.*, 2013; Thorstensson *et al.*, 2014; Bumba *et al.*, 2016). In previous studies, the secretion, release, binding to host cells, interaction with host cells, functional effects of ACT on host cells, and its role in establishing an infection have been characterized. This host-directed protein bacterial toxin has not, however, been studied for effects on the bacterium itself, and here we describe a novel function for ACT.

In the present work we have directly tested the hypothesis that the ACT-FHA interaction inhibits biofilm by adding purified ACT to cultures of *B. pertussis* and *B. bronchiseptica in vitro*. Indeed, exogenous ACT inhibits biofilm formation, adding to the effect of endogenously produced and secreted ACT. This effect of added ACT occurs through binding of the catalytic AC domain, independently of its enzyme activity, to the mature C-terminal domain (MCD) of FHA, which must be properly folded for the inhibitory effect of ACT to occur. The possible relationship of this novel regulatory role for a bacterial toxin to the hypothetical "life cycle" of *B. pertussis*, controlled by BvgAS, is discussed.

RESULTS

Exogenous ACT inhibits biofilm in a concentration-dependent manner

In light of the observation by Irie *et al.*, which showed that *B. bronchiseptica* Δ*cyaA* (RB58) produced more biofilm than WT, we tested the hypothesis that ACT has an inhibitory effect on *B. pertussis* biofilm as well. The *B. pertussis* mutant, BP348, lacking ACT by virtue of a transposon insertion in *cyaA*, and the parental WT strain, BP338, were compared for their abilities to form biofilm. BP338, BP348 and BP347 were grown in 96 well plates and biofilm formation was measured by bacterial accumulation on wells using the crystal violet assay. As shown in figure 1A, BP348 made more biofilm than BP338. Bvg(−) BP347, a negative control, formed no biofilm; the low, but measurable, OD_{595} reflects basal levels of bacterial adherence, and was previously observed for Bvg(−) *B. pertussis* (Mishra *et al.*, 2005). These differences in biofilm formation are not due to differences in bacteria growth, in 10 mL SSM shaking cultures all strains grew at the same rate, while under 100μL static culture conditions in 96 well plates, BP338 and BP348 grew at similar rates. BP347, which does not make biofilm, reached a higher OD_{600} more quickly (Figure S1), excluding impaired bacterial growth as the cause of differences in biofilm formation.

We next tested exogenous, purified, recombinant ACT for its ability to inhibit biofilm formation by *B. pertussis* and *B. bronchiseptica*. Exogenous ACT was added at concentrations of 10, 100 or 1000 ng mL^{-1} (56 pM, 565 pM, 5650 pM respectively) to BP338 cultures. The concentration-dependent inhibition of biofilm is demonstrated in Figure 1B (IC_{50} 17.32 ng ml^{-1} to reduce biofilm to negative control OD_{595}). *B. pertussis* grown in the presence of ACT or urea, a major component of the solution in which ACT is stored, grew at the same rate as in media alone, further showing that differences in growth rate do not account for reduced biofilm formation. (Figure S2). The same concentration-dependent inhibition of biofilm by ACT occurred with *B. bronchiseptica* (Figure S3A). Importantly, the concentrations of ACT (approximately 100 ng mL^{-1}) used in this study are comparable to calculated concentrations found in nasopharyngeal washes from baboons and infants infected with *B. pertussis* (Eby *et al.*, 2013).

The AC domain is necessary and sufficient for inhibition of biofilm

ACT is a 177 kDa, multi-domain protein, and to determine which part(s) of the ACT molecule are involved in the inhibitory effect, we tested truncated ACT variants and an ACT protein mutant lacking AC enzymatic activity (iACT) for their abilities to inhibit biofilm formation (Figure 1C is a schematic representation of modifications). These variants, which are partial deletions from full-length Δ*cyaA* (Sebo and Ladant, 1993; Sadilkova *et al.*, 2008), were previously used to characterize monoclonal antibodies (Lee *et al.*, 1999) and have been used previously in functional assays (Sakamoto *et al.*, 1992; Iwaki *et al.*, 1995; Macdonald-Fyall *et al.*, 2004; Eby *et al.*, 2014).

All ACT variants, with one exception, inhibited biofilm formation to the same extent as full-length ACT (Figure 1C). $ACT_{\Delta AC}$, ACT lacking the catalytic domain, was without an inhibitory effect at 100 ng mL^{-1}, while the 43 kDa AC domain was comparable to native ACT in inhibiting biofilm formation at just 10 ng mL^{-1} (comparable molar concentrations),

and did so in a concentration-dependent manner (Figure S4). iACT, the enzymatically inactive form of the toxin (1000-fold reduction in enzymatic activity in comparison to ACT holotoxin), inhibited biofilm comparably to ACT at 100 ng mL^{-1} (Figure 1D), establishing that the enzymatic activity of the toxin is not required for the inhibitory effect. Thus the AC domain is both necessary and sufficient for biofilm inhibition, yet its catalytic activity contained in the AC domain is not required.

The AC domain is the most conserved portion of ACT among *Bordetella* species that encode the toxin (Park *et al.*, 2012), indicating the possibility of a comparable inhibitory role for the AC domain in biofilm regulation among the *Bordetellae*. The AC domain is also necessary and sufficient to inhibit *B. bronchiseptica* RB50 biofilm (Figure S3B). To confirm the role of endogenous ACT and its catalytic domain, we constructed BP338 ΔAC. The portion of *cyaA* encoding the AC domain (Δ1–373) was deleted and the resultant strain, BP338 ΔAC, was tested for biofilm formation as in *in vitro* assays described above. A western blot was completed to show that the BP338 ΔAC mutant expresses truncated ACT peptide (Figure S5). As expected, BP338 ΔAC made more biofilm than the parental WT BP338 (Figure 1E), confirming the necessity for and specificity of the AC domain to inhibit biofilm in *B. pertussis*.

In that the crystal violet assay is an indirect quantification of biofilm, we used Scanning Electron Microscopy to determine the effects of AC domain on BP338 biofilm, using BP347 as a biofilm-negative control. We allowed *B. pertussis* to form biofilm on glass coverslips in the absence and presence of exogenous AC domain to complement data from the crystal violet assay. Samples obtained under these conditions were imaged using a Zeiss Sigma VP HD Field Emission Scanning Electron Microscope (SEM). Figure 2 illustrates the dramatic effects of AC domain under these conditions. WT BP338 (Figure 2A) and Bvg(−) BP347 (Figure 2B) biofilm were compared to BP338 grown in the presence of 10 ng mL^{-1} AC domain (Figure 2C). The exogenous AC domain precluded biofilm accumulation on glass coverslips, such that BP338 plus AC domain was equivalent to the negative control, BP347. In the images of BP347 and BP338 plus AC domain, there are few bacteria adherent to the coverslip. The lack of bacterial accumulation under these conditions suggests a defect in the initial binding of bacteria, which then impairs subsequent biofilm accumulation. Thus, the initial step of binding to the abiotic surface would be one determinant of the ability of *B. pertussis* to produce robust biofilm.

AC domain inhibits bacterial aggregation and disrupts preformed B. pertussis biofilm

To address the underlying mechanisms of ACT inhibition of biofilm, we tested other steps in the biofilm life cycle for susceptibility to ACT inhibition. Bacterial aggregates form in shaking culture and positively correlate with biofilm formation in many bacterial species (Sorroche *et al.*, 2012; Kragh *et al.*, 2016). Exogenous AC domain was added to growing cultures of *B. pertussis* and the aggregation index was determined at 24 hours, as previously described for *B. pertussis* (Arnal *et al.*, 2015). Exogenous AC domain decreased bacteria aggregation by 75% (Figure 3A).

The final stages of the biofilm lifecycle involve dispersal of the bacteria from the biofilm structure. In order to investigate further the regulatory effect of ACT on biofilm, we tested

the effect of AC domain when added to existing biofilm. Figure 3B shows the time course of biofilm formation in the presence (red solid line) and absence of AC domain (black solid line). When AC domain was added to BP338 biofilm at 72 hours post inoculation and measured 24 hours later (96 hours), biofilm formation was reduced 76% (blue dotted line) compared to BP338 alone at 96 hours, resulting in quantities comparable to biofilm formed in the continuous presence of AC domain (red line). This disruption of existing biofilm did not occur when full-length ACT was added at 72 hours (data not shown). Although we do not know the mechanism of disruption, we hypothesize that the lack of effect of ACT was due to limitations in the ability of the large hydrophobic protein to access the necessary site(s) within the biofilm. Collectively, these data suggest that ACT plays several roles in regulation of *Bordetella* biofilm, not only during the initial steps, but also during later stages.

The inhibition of biofilm formation by ACT is specific

To characterize the inhibitory effects of exogenous ACT and AC domain on *B. pertussis* biofilm formation, we tested molecules that interact with ACT for their ability to affect ACT-mediated inhibition. Calmodulin (CaM) binds the AC domain of ACT with high affinity (K_d ~2 nM) and activates its enzymatic activity (Guo *et al.*, 2005). It has been previously demonstrated that addition of CaM to ACT, prior to incubation with cells, blocks translocation of the AC domain into the cell cytosol, thereby precluding cAMP production (Mouallem *et al.*, 1990; Gray *et al.*, 2001). In the present studies, purified ACT or AC domain and CaM were combined before addition to bacteria. Under these conditions, a molar excess of CaM prevented the inhibitory effect of ACT or AC domain on biofilm formation (Figure 4). Similarly, an antibody directed against the catalytic domain of ACT blocked the inhibitory effects of ACT and AC domain on biofilm (Figure 4). The fact that CaM or an antibody blocks the inhibitory effect of ACT suggests the possibility that CaM causes a disruption of a physical interaction between ACT and another bacterial factor, such as filamentous hemagglutinin (FHA), which is involved in biofilm formation.

The AC domain interacts with FHA

In a *B. pertussis* mutant lacking FHA, ACT is present in the media as opposed to remaining surface-associated (Weiss *et al.*, 1983) and ACT interacts with FHA on the surface of bacteria (Zaretzky *et al.*, 2002). These data led us to the hypothesis that ACT directly interacts with FHA to inhibit biofilm formation. In light of this collection of observations and the fact that AC domain is necessary and sufficient for inhibition of biofilm, we explored the interaction of the AC domain with FHA by surface plasmon resonance (SPR).

The FHA (~220 kDa) protein, purified from *B. pertussis* culture supernatant (Figure S6), was immobilized on GLC sensor chip and real-time kinetics of the interaction of the recombinant AC domain with FHA was analyzed by parallel injection of diluted AC protein over the sensor chip surface at a constant flow rate of 30 μl/min (Figure 5A). Interaction of the AC domain with FHA was specific, since negligible binding of the AC domain was observed to the chip coated with FHA44, a truncated FHA protein corresponding to residues 72–862 of FHA, which does not contain the c-terminal domain (Figure 5B). Kinetic parameters of the AC-FHA interaction were calculated from global fitting of concentration-dependent binding curves. As shown in Figure 5A, the binding curves fit well to a

Langmuir-type binding model indicating a simple 1:1 interaction between the AC domain and FHA with equilibrium dissociation constant (K_D) of approximately 650 nM. These data suggest that the AC domain only interacts with FHA when c-terminal segment is present.

To complement the functional data which shows CaM blocks the inhibitory effects of AC domain on biofilm formation, AC domain was mixed with CaM in molar ratios of 10:1, 1:1 or 1:10 and the capacity of AC domain-CaM complex to interact with FHA was probed by SPR. As shown in Figure 5C, binding of the AC domain to FHA in the presence of CaM (10:10) was reduced approximately 75% as compared to AC domain alone, suggesting that CaM and FHA compete for the same site on AC domain, or that CaM binding alters conformation of the AC domain thereby interfering with the ACT-FHA interaction. The data presented in Figure 4 show that an excess of CaM blocks AC domain inhibition of biofilm and the data in Figure 5C show that equal molar ratios of AC domain:CaM reduce binding to FHA by 75%. Based on these data we hypothesized that the molar excess of CaM used in the biofilm assay blocks the inhibitory effects of ACT on biofilm formation by blocking the physical interaction between ACT and FHA.

In that the c-terminal portion of FHA is required for AC domain binding to FHA (Figure 5B, FHA44), we hypothesized that ACT and the AC domain would block specific antibody interactions with FHA. To test this hypothesis, we developed an ELISA-based assay to characterize the interaction between ACT and the c-terminal segment of FHA. Plates were coated with full length FHA and incubated with buffer, ACT, or AC domain over a range of concentrations (0.1–10 μg mL^{-1}), or $ACT_{\Delta AC}$ at 10 μg mL^{-1}. Monoclonal antibodies directed against the mature C-terminal domain (MCD) of FHA (residues 1870–2362) were used to determine the accessibility of the c-terminal segment of FHA. This anti-MCD antibody has been used previously to detect FHA and study FHA processing (Mazar and Cotter, 2006; Noel *et al.*, 2012), and was used in this study because it recognizes a large portion of FHA that was deleted from the truncated FHA44 mutant protein.

The presence of ACT or AC domain blocked anti-MCD antibodies from binding to FHA (Figure 6). Both ACT and the AC domain produced a concentration-dependent inhibition of anti-MCD antibody binding to FHA, but, in accordance with the earlier functional data on inhibition of biofilm, $ACT_{\Delta AC}$ had no effect (Figure 6). Furthermore, incubation of ACT or the AC domain with CaM prior to addition to FHA-coated plates precluded them from blocking the binding of MCD antibody to FHA (striped bars, Figure 6). Because the data regarding ACT inhibition of biofilm correlate with the physical binding of the AC domain and FHA, the consequences of their physical interaction were investigated to better understand the molecular mechanisms involved in biofilm inhibition.

The MCD of FHA is required for ACT inhibition of biofilm

FHA is delivered to the bacterial surface via a two-partner secretion pathway. This process involves translocation of FhaB, the FHA precursor, through FhaC, an FhaB-specific outer-membrane transporter (Fan *et al.*, 2012). FhaB enters the FhaC channel as a hairpin and then begins folding in an N-to-C-terminal manner on the cell surface, creating a β-helical shaft (Mazar and Cotter, 2006; Mazar and Cotter, 2007). After the region distal to the β-helical shaft reaches the cell surface, the C-terminal prodomain is proteolyzed in the periplasm,

creating the “mature C-terminal domain” (MCD), which is located on the distal portion of FHA (Noel *et al.*, 2012). To better understand the functional domains involved in ACT binding and inhibition of biofilm, we studied *B. pertussis* and *B. bronchiseptica* mutants with altered secretion and processing of FHA.

Since the MCD of FHA is required for AC domain binding (Figure 5B), we hypothesized that the MCD must be present in order for ACT inhibition to occur. A *B. pertussis* mutant lacking the MCD was assessed for biofilm formation in the presence and absence of ACT to determine the role of the MCD in the inhibitory process. BPSM JS20, a derivative of parental strain BPSM, produces a truncated FHA by virtue of deletion of the MCD and C-terminal prodomain and, is therefore, composed only of the β-helical shaft. BPSM and BPSM JS20 were grown in the presence and absence of ACT and biofilm formation was measured at 96 hours. WT BPSM formed biofilm that was susceptible to inhibition by ACT. Importantly, the BPSM isogenic strain and the BP338 isogenic strain, both of which are Tohama I derivatives, were compared for biofilm formation, ACT expression and FHA expression. No significant differences were observed in biofilm formation between the parental WT strains (Figure S7A). FHA protein expression was similar between the two strains, although there was slightly more ACT protein expression in BPSM. (Figure S7B). BPSM JS20 formed equivalent amounts of biofilm in the presence and absence of exogenous ACT (Figure 7A) and made more biofilm than the parental BPSM strain in the absence of exogenous ACT; this may be due to the inability of endogenous ACT to have an effect on BPSM JS20 biofilm. The equivalent BPSM JS20 mutant strain in *B bronchiseptica*, which is derived from RBX11 and lacks the MCD and C-terminal prodomain, produced biofilm that is not inhibited by ACT (Figure S8). Although the MCD is not required for biofilm formation, it appears to be necessary for ACT-mediated inhibition of biofilm to occur. These data are consistent with the SPR results showing ACT does not bind FHA44, which lacks the MCD (Figure 5B).

To validate the role of the MCD in ACT inhibition of biofilm, we tested a mutant in which the MCD is improperly folded. BPSM T-N, also derived from BPSM parental WT strain, contains a mutation in *fhaB* such that a stop codon is introduced in the region encoding the N-terminus of the prodomain. As a result, the MCD is present and located distally from the cell surface, but is not folded in its native conformation (Mazar and Cotter, 2006; Noel *et al.*, 2012). BPSM T-N formed similar amounts of biofilm compared to BPSM, yet like BPSM JS20, ACT did not inhibit biofilm formation of this strain (Figure 7A). The same was true for RBX11 T-N, the equivalent *B. bronchiseptica* strain with a misfolded MCD (Figure S8). Although the MCD itself is not required for biofilm formation, the MCD of FHA must be present and in the proper conformation for the inhibition of biofilm by ACT to occur. These data directly link the ACT-FHA interaction to inhibition of biofilm by ACT in *B. pertussis* and *B. bronchiseptica*.

In light of the inhibitory effects of ACT and the fact that ACT and anti-MCD antibody both bind to the MCD, the ability of the anti-MCD antibody to block biofilm was tested. Indeed, when BP338 was grown in the presence of anti-MCD antibodies, there was a reduction in biofilm (Figure 7B). These data suggest that the anti-MCD antibody may block biofilm formation in a similar manner to ACT, support the competition between the ACT and the

anti-MCD antibodies for FHA binding, and corroborate previous studies showing that polyclonal antibodies directed against FHA block biofilm formation (Serra *et al.*, 2011). It is clear that the MCD of FHA plays a part in inhibition of biofilm, although its exact role is unclear. When binding partners, either anti-MCD antibodies or the AC domain, are present, biofilm formation is inhibited. Further investigation of the MCD and its role in regulating biofilm will be important to understand *Bordetella* biofilm and the effects of ACT.

DISCUSSION

The data presented here link the ACT-FHA interaction to inhibition of biofilm formation by *Bordetella pertussis* and *Bordetella bronchiseptica in vitro*. The AC domain is necessary and sufficient, yet the catalytic activity of the toxin is not required for this inhibitory phenomenon. These effects of ACT can be blocked by CaM or by a catalytic domain-specific antibody. We have identified the AC domain as a sufficient binding partner for FHA, and the MCD as necessary for this binding and the inhibitory effect on biofilm to occur. The inhibitory effect may result from the AC domain – MCD interaction simply blocking the FHA molecule in its yet-to-be-identified role in *Bordetella* biofilm production, or by inducing a conformational change in FHA that has this and other effects. Our working model for the inhibition of *B. pertussis* biofilm by ACT is diagrammed in Figure 8; the AC domain of ACT binds the MCD of FHA to interfere with inter-bacterial FHA-FHA interactions, which have been previously described as important for biofilm formation. The inhibition by ACT may start in the early steps of biofilm formation, by ACT blocking initial bacteria-substrate, as well as bacteria-bacteria interactions and thus limiting subsequent biofilm accumulation. We have, however, been unable to relate our data to the observations by Perez Vidakovics *et al.* showing that the absence of ACT reduces *B. pertussis* binding to alveolar epithelial cells (Perez Vidakovics *et al.*, 2006).

Our data illustrating inhibition of *Bordetella* biofilm by ACT through its interaction with FHA raise the important question of how this phenomenon fits with the current concepts of *Bordetella* pathogenesis and biofilm production. Others have shown that multiple factors, ranging from (p)ppGpp and c-di-GMP to transcriptional regulators of Bps polysaccharide production, control biofilm production by *Bordetellae* (Conover *et al.*, 2012; Sugisaki *et al.*, 2013; Sisti *et al.*, 2013). Specifically, Irie *et al.* and Mishra *et al.* demonstrated that BvgAS modulates the formation of biofilm and that there is an increase in *B. bronchiseptica* biofilm under Bvg(i) conditions (Irie *et al.*, 2004). This scenario can now be explained, at least in part, by a reduction in the amount of inhibitory ACT in the presence of a constant level of FHA in the Bvg(i) phase (Cotter and Miller, 1997; Mattoo and Cherry, 2005; Vergara-Irigaray *et al.*, 2005). Thus, during active phase of infection in which conditions are optimal for the bacteria, ACT is actively produced for its inhibitory effects on the host immune response and biofilm production is suppressed (Figure 8). Under less favorable conditions, during which a defensive posture might be beneficial, a reduction in ACT production could be one of several mechanisms by which production of biofilm is initiated.

Given the active production of ACT during the Bvg(+) phase, it is appropriate to ask why there is any biofilm produced during these *in vitro* assays. We now know that the quantity and distribution of ACT is different than what occurs *in vivo*. Previously, we have

demonstrated that in *ex vivo* samples obtained during active infection, concentrations of ACT can reach approximately 100 ng mL^{-1} and all of the ACT is in the supernatant fraction, as opposed to being surface associated (Eby *et al.*, 2013). This is in contrast to *B. pertussis* cultured *in vitro* in SSM, in which >90% of the ACT remains surface-associated and concentrations rarely get as high as seen in the *ex vivo* samples (Eby *et al.*, 2013). We have also shown that the functional form of the toxin is that which is released into the media (Gray *et al.*, 2004), while the surface-associated toxin is likely an improperly folded, inert pool.

Finally, this is not the first report of a single protein having multiple, seemingly unrelated biochemical functions. Dr. Constance Jeffery has described and catalogued (www.moonlightingproteins.org) a number of dual function protein molecules, in which a single protein performs multiple physiologically relevant biochemical or biophysical roles (Jeffery, 1999; Jeffery, 2003; Jeffery, 2009; Jeffery, 2014; Jeffery, 2015). On the basis of recognizing additional functions for known proteins, these fascinating molecules, which are from both prokaryotic and eukaryotic sources, have been designated “moonlighting proteins”. Their study has enabled identification of novel biochemical pathways and protein functions, and allowed systems biologists to better understand cellular processes. Prior to this study, ACT has been studied and characterized solely a host-directed protein bacterial toxin, that modulates function and is cytotoxic for some target cells by increasing cAMP levels and, depending on concentration, depleting ATP levels. ACT is also a hemolysin and member of the RTX family of pore-forming toxins, which includes *E. coli* hemolysin, HlyA (Menestrina *et al.*, 1994). The pore-forming function, which for ACT is involved in delivery of its catalytic domain to the target cell interior, has an additional effect of compromising membrane integrity and polarization and contributes to cytotoxicity. The additional role for this protein bacterial toxin, contained within its catalytic domain, namely interaction with a surface adhesion to impair formation of biofilm makes it unlike any other moonlighting protein that has been described in the Moonprot database (Mani *et al.*, 2015). This information can now be used to study *Bordetella* biofilm and to hypothesize when formation may occur *in vivo*. The ability of ACT to inhibit biofilm needs to be investigated further to understand the therapeutic and prophylactic implications. Additionally this information may provide a building block for future studies that elucidate similar novel functions in other bacterial protein toxins.

EXPERIMENTAL PROCEDURES

Bacterial Strains and Growth Conditions

B. pertussis WT BP338 (Tohama I); Bvg(−) BP347 (TN5::*bvgS* mutant derived from BP338); WT BPSM (Tohama I); BPSM JS20 (*fhaB* ΔMCD and C-terminal prodomain derivative of BPSM); and BPSM T-N (*fhaB* with transposon insertion in C-terminal prodomain derivative of BPSM) were grown on Bordet-Gengou (BG) agar (Gibco) supplemented with 15% defibrinated sheep blood (Cocalico) for 48 hours at 37°C. The same growth conditions were used for *B. bronchiseptica* strains, WT RB50; Bvg(−) RB54; RBX11-JS20 (*fhaB* ΔMCD and C-terminal prodomain); and RBX11 T-N (*fhaB* with transposon insertion in C-terminal domain). These *B. pertussis* strains have been previously

reported (Weiss *et al.*, 1983; Mazar and Cotter, 2006), as have *B. bronchiseptica* strains (Mazar and Cotter, 2006). Bacteria were then transferred to liquid culture in modified synthetic Stainer-Scholte liquid medium (SSM) and grown for 24 hours at 37°C, shaking at 150 RPM. Bacteria were pelleted and washed in SSM, and then resuspended to an OD_{600} of 0.1 for biofilm experiments.

Strain Construction (ΔAC domain)

Two DNA fragments (517 and 513 bps), corresponding to the 5 and the 3 flanking region of the in-frame deletion, were amplified from B. pertussis genomic DNA as a template by PCR using two pairs of primers

F1: 5-TTTACTAGTGGGATTGAGGAGGGAGGGC-3;

R1: 5-TTTATGCATGTGGATCTGTCGATAAGTAGTC −3

F2: 5-TTTATGCATAAGTTCTCGCCGGATGTACTG −3;

R2: 5-TTTGAATTCGCCGCCTCCCAGCGCCAT −3

The primers were cut with the SpeI/NsiI and NsiI/EcoRI, respectively, and ligated with the SpeI/EcoRI-cleaved pSS4245 vector. Bacteria were mated following the previously described methods for *B. pertussis* . Briefly, *B. pertussis* BP338 was passaged 2–3 days on BG and grown over night in SSM. The OD_{600} was between 0.7 and 0.8. RHO3 *E. coli* were grown in antibiotic selection media, LB + 150 μg mL^{-1} ampicillin (AMP) supplemented with 400 μg mL^{-1} DAP to mid-log phase. A 2:1 donor to recipient ratio was used. After washing, the bacteria were resuspended in 100 μL SSM and plated on BG + $MgSO_4$ + DAP plates. After an overnight incubation (approximately 15 hours), the plates were swabbed, the material was washed to remove residual DAP and resuspended in 100 μL SSM. Bacteria were plated on BG + $MgSO_4$ + AMP. Colonies were isolated and confirmed to lack the AC domain via western blot and PCR.

ACT and ACT Mutant Protein Purification

As previously described, calmodulin columns were used to isolate holotoxin ACT from whole-cell urea extracts of XL1-Blue *E. coli* transformed with plasmid *pT7cACT1*. Similar methods were used to purify the ACT deletion mutants expressed from the previously described plasmid constructs with similar backbone, whole-cell urea extracts of XL1-Blue *E. coli* transformed with the following plasmids and urea-extracted material was used in assays described below; $ACT_{\Delta AC}$ (pCACT Δ-373), $ACT_{\Delta HR}$ (pCACT Δ385–1489), $ACT_{\Delta H}$ (pCACT Δ385–1006), $ACT_{\Delta R}$ (pCACT ΔC217), and iACT (pGW44/188) (Lee *et al.*, 1999). The AC domain was purified from the *E. coli* BL21 (λDE3) strain expressing the AC-int-CBD fusion protein (Sadilkova *et al.*, 2008). Briefly, bacteria were grown at 30°C in MDO medium supplemented with 150 mg mL^{-1} of ampicillin. Cultures were induced with IPTG (1 mM), the cells were washed and resuspended in 50 mM Tris-HCl (pH 7.4), 150 mM NaCl (TN buffer) containing 1 mM EDTA (EDTA buffer), and disrupted by sonication. For protein purification by chitin affinity chromatography, the cell extract was cleared at 20,000 × g and loaded on a chitin bead column. After washing, EDTA buffer containing 50 mM dithiothreitol was loaded on the column to promote self-excision of the intein-CBD from the AC-intein-CBD fusion protein during overnight incubation at 4°C. The AC domain was then

eluted with EDTA buffer and dithiothreitol was removed by dialysis against TN buffer. Purified proteins were stored at −70°C until use.

FHA and FHA44 purification

FHA was produced using *B. pertussis* Tohama I, while *B. pertussis* Fha44-stop was used to produce the ~80 kDa N-terminal fragment of FHA that comprises residues 72 to 862 of FhaB (the fhaB allele having a stop codon inserted at position 863 was constructed according to Renaud-Mongenie. Bacteria were grown in 1 L shaking liquid cultures in SSM supplemented with 1 g L^{-1} of (2,6-O-dimethyl)-β-cyclodextrin (Sigma). At OD600nm ≥ 4.0, culture supernatants were collected by centrifugation at 10,000 x g for 20 minutes at 4°C and were sterilized by passage through filters with 0.22 μm pore diameter before loading onto 5 ml Cellufine sulphate columns (JNC corporation) equilibrated with 10 mM sodium phosphate buffer at pH 7.6 (buffer A). After sample application, both matrices containing adsorbed FHA or FHA44 were washed with 80 column volumes (cv) of buffer A, after which a second wash of 20 cv was performed with buffer A containing 300 mM NaCl. The purified FHA and FHA44 proteins were eluted with 700 mM NaCl in buffer A and were stored frozen at – 70°C until use. The entire purification procedure on chromatography column was performed at 4°C.

Microtiter Crystal Violet Assay

Bordetella biofilm was measured using the microtiter plate assay, coupled with crystal violet staining, as previously described (O'Toole, 2011). Briefly, *Bordetella* bacteria were grown in a total volume of 100 μL of Stainer-Scholte medium at 37°C in 96-well polyvinylchloride (PVC), round-bottom, non-tissue-culture treated microtiter plates (NuncBrand). *B. pertussis* biofilm was measured at 96 hours and *B. bronchiseptica* biofilm was measured at 72 hours. Wells were washed at the final time point to remove planktonic bacteria. Bacterial cells that remained attached to the wells were stained with a 0.1% solution of crystal violet (CV) and were incubated at room temperature for 30 min. The washing process was repeated, and the CV stain was solubilized from bacterial cells with 200 μl of 95% ethanol. Biofilm formation was quantitated by measuring OD_{595}.

Scanning Electron Microscopy

Biofilms were grown statically in 24-well non-tissue culture treated polypropylene plates (0.5 mL cultures per well), and a circular microscope cover glass (12CIR.-1.5) was inserted into each well. Bacteria successfully adhered to the coverslip, as initially confirmed by Gram stain, and matrix was present as determined by Calcofluor White staining. Coverslips were placed in 4% paraformaldehyde to fix samples. *B. pertussis* biofilm was observed on the surfaces of the coverslips at 96 hours under various conditions.

Aggregation Assay

Bacterial aggregation was measured using previously described methods for *B. pertussis* (Arnal *et al.*, 2015). Briefly, BP338 was grown in the presence and absence of AC domain for 24 hours at 37°C shaking. At 24 hours, six 1 mL samples were collected. Three were homogenized by vigorous vortexing and three were not homogenized before centrifugation

at 650 x g for 2 min. The OD_{600} was then measured from the supernatant, and the aggregation index (AI) was calculated based on the following equation: $(OD_{homogenized} - OD_{nonhomogenized})/OD_{homogenized}$. Three independent experiments were performed in triplicate.

Surface Plasmon Resonance

SPR measurements were performed at 25°C using a ProteOn XPR36 Protein Interaction Array System (Bio-Rad, Hercules, CA, USA). FHA and FHA44 were diluted to a final concentration of 1 μg mL^{-1} in PBS containing 0.005 % Tween-20 and immobilized as ligands to a GLC sensor chip (Bio-Rad) at flow rate of 30 μl/min. SPR measurements were carried out in the running buffer containing PBS supplemented with 0.005% Tween-20 at the flow rate of 30 μL min^{-1} for association and dissociation phase of sensograms. The purified AC domain was diluted in the running buffer to the indicated concentrations and injected in parallel ("one-shot kinetics") over the chip surface. The sensograms were corrected for sensor background by interspot referencing (the sites within the 6 × 6 array which are not exposed to ligand immobilization but are exposed to analyte flow), and double referenced by subtraction of analyte (channels 1–5) using a "blank" injection (channel 6). The data were analyzed globally by fitting both the association and the dissociation phases simultaneously for five different AC domain concentrations using a 1:1 Langmuir-type binding model. An apparent equilibrium dissociation constant (K_D) was determined as $K_D=k_d/k_a$.

ELISA-based Binding Assay

ELISA-specific MaxiSorp 96-well immunoplates (Thermo Scientific) were coated with 0.5 μg mL^{-1} FHA overnight in 100μL bicarbonate solution. Before beginning the assay, the wells were washed and then blocked in 5% milk 1X PBS 0.05% Tween for 1 hour. Wells were washed and control (no protein), ACT, AC domain or $ACT_{\Delta AC}$ (50 μL) was added for 30 minutes. Anti-MCD antibodies described previously (Noel *et al.*, 2012) (50 μL of 1:100,000 dilution) were added to wells for 30 minutes after the addition of the first 50 μL solution. Wells were washed and a secondary anti-rabbit-HRP linked antibody was added to wells for 1 hour. Wells were washed again and the detection solution (SureBlue TMB Microwell Peroxidase Substrate) was added for fifteen minutes. HCl 1N was added to stop the detection solution reaction and the absorbance at OD_{450} was read using an uQuant Bio-Tek ELISA reader.

Statistics

Statistical analysis was performed using student's unpaired t test with Welch's correction, assuming Gaussian distribution (parametric test), these tests were performed on data sets to compare conditions within experiments.

Supplementary Material

Refer to Web version on PubMed Central for supplementary material.

Acknowledgments

We would like to thank Rajendor Deora at Wake Forest University for providing background knowledge and guidance in studying *Bordetella* biofilm and Pamela Schaefer of the University of Virginia for all of her administrative help. The Advanced Microscopy Facility at the University of Virginia was a much appreciated resource, specifically Yalin Wang and Stacey Guillot. We would also like to thank members of Peter Sebo's lab, specifically Ladislav Bumba, Radim Osicka, and Rodrigo Villarino Romero, who completed Surface Plasmon Resonance experiments that have been included in the manuscript. This work was supported by the NIH/NIAID Grant AI18000 - Erik L. Hewlett at University of Virginia, University of Virginia's Infectious Disease Training Grant NIH/NIAID AI007046-38 – Casandra Hoffman at University of Virginia, NIH Grant AI094991 - Peggy A. Cotter at University of North Carolina, and Grants No 13-14547S – Peter Sebo and No GA15-09157S – Radim Osicka from the Science Foundation of The Czech Republic.

REFERENCES

Arnal L, Grunert T, Cattelan N, de Gouw D, Villalba MI, Serra DO, et al. *Bordetella pertussis* Isolates from Argentinean Whooping Cough Patients Display Enhanced Biofilm Formation Capacity Compared to Tohama I Reference Strain. Front Microbiol. 2015; 6:1352. [PubMed: 26696973]

Basler M, Masin J, Osicka R, Sebo P. Pore-forming and enzymatic activities of *Bordetella pertussis* adenylate cyclase toxin synergize in promoting lysis of monocytes. Infect Immun. 2006; 74:2207–2214. [PubMed: 16552051]

Birkebaek NH, Kristiansen M, Seefeldt T, Degn J, Moller A, Heron I, et al. *Bordetella pertussis* and chronic cough in adults. Clin Infect Dis. 1999; 29:1239–1242. [PubMed: 10524969]

Bisgard KM, Pascual FB, Ehresmann KR, Miller CA, Cianfrini C, Jennings CE, et al. Infant pertussis: who was the source? Pediatr Infect Dis J. 2004; 23:985–989. [PubMed: 15545851]

Bumba L, Masin J, Fiser R, Sebo P. *Bordetella* adenylate cyclase toxin mobilizes its beta2 integrin receptor into lipid rafts to accomplish translocation across target cell membrane in two steps. PLoS Pathog. 2010; 6:e1000901. [PubMed: 20485565]

Bumba L, Masin J, Macek P, Wald T, Motlova L, Bibova I, et al. Calcium-Driven Folding of RTX Domain beta-Rolls Ratchets Translocation of RTX Proteins through Type I Secretion Ducts. Mol Cell. 2016; 62:47–62. [PubMed: 27058787]

Cherry, JD.; Heinninger, U. Textbook of Pediatric Diseases Pertussis and other Bordetella infections. The W.B. Saunders Co; 2004. Pertussis and other *Bordetella* infections; p. 1588

Cherry JD, Olin P. The science and fiction of pertussis vaccines. Pediatrics. 1999; 104:1381–1383. [PubMed: 10585991]

Confer DL, Eaton JW. Phagocyte impotence caused by an invasive bacterial adenylate cyclase. Science. 1982; 217:948–950. [PubMed: 6287574]

Conover MS, Mishra M, Deora R. Extracellular DNA is essential for maintaining *Bordetella* biofilm integrity on abiotic surfaces and in the upper respiratory tract of mice. PLoS One. 2011; 6:e16861. [PubMed: 21347299]

Conover MS, Redfern CJ, Ganguly T, Sukumar N, Sloan G, Mishra M, Deora R. BpsR modulates *Bordetella* biofilm formation by negatively regulating the expression of the Bps polysaccharide. J Bacteriol. 2012; 194:233–242. [PubMed: 22056934]

Conover MS, Sloan GP, Love CF, Sukumar N, Deora R. The Bps polysaccharide of *Bordetella pertussis* promotes colonization and biofilm formation in the nose by functioning as an adhesin. Mol Microbiol. 2010; 77:1439–1455. [PubMed: 20633227]

Costache A, Bucurenci N, Onu A. Adenylate cyclases involvement in pathogenicity, a minireview. Roum Arch Microbiol Immunol. 2013; 72:63–86. [PubMed: 23947014]

Cotter PA, Miller JF. A mutation in the *Bordetella bronchiseptica* bvgS gene results in reduced virulence and increased resistance to starvation, and identifies a new class of Bvg-regulated antigens. Mol Microbiol. 1997; 24:671–685. [PubMed: 9194696]

de Gouw D, Serra DO, de Jonge MI, Hermans PW, Wessels HJ, Zomer A, et al. The vaccine potential of *Bordetella pertussis* biofilm-derived membrane proteins. Emerg Microbes Infect. 2014; 3:e58.

Eby JC, Ciesla WP, Hamman W, Donato GM, Pickles RJ, Hewlett EL, Lencer WI. Selective translocation of the *Bordetella pertussis* adenylate cyclase toxin across the basolateral membranes of polarized epithelial cells. J Biol Chem. 2010; 285:10662–10670. [PubMed: 20139088]

Eby JC, Gray MC, Hewlett EL. Cyclic AMP-mediated suppression of neutrophil extracellular trap formation and apoptosis by the *Bordetella pertussis* adenylate cyclase toxin. Infect Immun. 2014; 82:5256–5269. [PubMed: 25287922]

Eby JC, Gray MC, Mangan AR, Donato GM, Hewlett EL. Role of CD11b/CD18 in the process of intoxication by the adenylate cyclase toxin of *Bordetella pertussis* . Infect Immun. 2012; 80:850–859. [PubMed: 22144488]

Eby JC, Gray MC, Warfel JM, Paddock CD, Jones TF, Day SR, et al. Quantification of the adenylate cyclase toxin of *Bordetella pertussis* in vitro and during respiratory infection. Infect Immun. 2013; 81:1390–1398. [PubMed: 23429530]

El-Azami-El-Idrissi M, Bauche C, Loucka J, Osicka R, Sebo P, Ladant D, Leclerc C. Interaction of *Bordetella pertussis* adenylate cyclase with CD11b/CD18: Role of toxin acylation and identification of the main integrin interaction domain. J Biol Chem. 2003; 278:38514–38521. [PubMed: 12885782]

Fan E, Fiedler S, Jacob-Dubuisson F, Muller M. Two-partner secretion of gram-negative bacteria: a single beta-barrel protein enables transport across the outer membrane. J Biol Chem. 2012; 287:2591–2599. [PubMed: 22134917]

Fedele G, Bianco M, Ausiello CM. The virulence factors of *Bordetella pertussis:* talented modulators of host immune response. Arch Immunol Ther Exp (Warsz). 2013; 61:445–457. [PubMed: 23955529]

Fenwick, BW. Bordetella. In: McVey, SD.; Kennedy, M.; Chengappa, MM., editors. Vetrinary Microbiology. Wiley-Blackwell; 2013. Section 14

Fiser R, Masin J, Bumba L, Pospisilova E, Fayolle C, Basler M, et al. Calcium influx rescues adenylate cyclase-hemolysin from rapid cell membrane removal and enables phagocyte permeabilization by toxin pores. PLoS Pathog. 2012; 8:e1002580. [PubMed: 22496638]

Gray MC, Donato GM, Jones FR, Kim T, Hewlett EL. Newly secreted adenylate cyclase toxin is responsible for intoxication of target cells by *Bordetella pertussis*. Mol Microbiol. 2004; 53:1709–1719. [PubMed: 15341649]

Gray MC, Lee SJ, Gray LS, Zaretzky FR, Otero AS, Szabo G, Hewlett EL. Translocation-specific conformation of adenylate cyclase toxin from *Bordetella pertussis* inhibits toxin-mediated hemolysis. J Bacteriol. 2001; 183:5904–5910. [PubMed: 11566989]

Guermonprez P, Khelef N, Blouin E, Rieu P, Ricciardi-Castagnoli P, Guiso N, et al. The adenylate cyclase toxin of *Bordetella pertussis* binds to target cells via the alpha(M)beta(2) integrin (CD11b/CD18). J Exp Med. 2001; 193:1035–1044. [PubMed: 11342588]

Guo Q, Shen Y, Lee YS, Gibbs CS, Mrksich M, Tang WJ. Structural basis for the interaction of *Bordetella pertussis* adenylyl cyclase toxin with calmodulin. EMBO J. 2005; 24:3190–3201. [PubMed: 16138079]

Hewlett EL, Donato GM, Gray MC. Macrophage cytotoxicity produced by adenylate cyclase toxin from *Bordetella pertussis*: more than just making cyclic AMP! Mol Microbiol. 2006; 59:447–459. [PubMed: 16390441]

Irie Y, Mattoo S, Yuk MH. The Bvg virulence control system regulates biofilm formation in *Bordetella bronchiseptica*. J Bacteriol. 2004; 186:5692–5698. [PubMed: 15317773]

Iwaki M, Ullmann A, Sebo P. Identification by in vitro complementation of regions required for cell-invasive activity of *Bordetella pertussis* adenylate cyclase toxin. Mol Microbiol. 1995; 17:1015–1024. [PubMed: 8594322]

Jeffery CJ. Moonlighting proteins. Trends Biochem Sci. 1999; 24:8–11. [PubMed: 10087914]

Jeffery CJ. Moonlighting proteins: old proteins learning new tricks. Trends Genet. 2003; 19:415–417. [PubMed: 12902157]

Jeffery CJ. Moonlighting proteins--an update. Mol Biosyst. 2009; 5:345–350. [PubMed: 19396370]

Jeffery CJ. An introduction to protein moonlighting. Biochem Soc Trans. 2014; 42:1679–1683. [PubMed: 25399589]

Jeffery CJ. Why study moonlighting proteins? Front Genet. 2015; 6:211. [PubMed: 26150826]

Kragh KN, Hutchison JB, Melaugh G, Rodesney C, Roberts AE, Irie Y, et al. Role of Multicellular Aggregates in Biofilm Formation. MBio. 2016; 7:e00237–e00216. [PubMed: 27006463]

Lee SJ, Gray MC, Guo L, Sebo P, Hewlett EL. Epitope mapping of monoclonal antibodies against *Bordetella pertussis* adenylate cyclase toxin. Infect Immun. 1999; 67:2090–2095. [PubMed: 10225859]

Lim A, Ng JK, Locht C, Alonso S. Protective role of adenylate cyclase in the context of a live pertussis vaccine candidate. Microbes Infect. 2014; 16:51–60. [PubMed: 24140230]

Macdonald-Fyall J, Xing D, Corbel M, Baillie S, Parton R, Coote J. Adjuvanticity of native and detoxified adenylate cyclase toxin of *Bordetella pertussis* towards co-administered antigens. Vaccine. 2004; 22:4270–4281. [PubMed: 15474718]

Mani M, Chen C, Amblee V, Liu H, Mathur T, Zwicke G, et al. MoonProt: a database for proteins that are known to moonlight. Nucleic Acids Res. 2015; 43:D277–D282. [PubMed: 25324305]

Martin C, Gomez-Bilbao G, Ostolaza H. *Bordetella* adenylate cyclase toxin promotes calcium entry into both CD11b+ and CD11b- cells through cAMP-dependent L-type-like calcium channels. J Biol Chem. 2010; 285:357–364. [PubMed: 19875442]

Mattoo S, Cherry JD. Molecular pathogenesis, epidemiology, and clinical manifestations of respiratory infections due to *Bordetella pertussis* and other *Bordetella* subspecies. Clin Microbiol Rev. 2005; 18:326–382. [PubMed: 15831828]

Mazar J, Cotter PA. Topology and maturation of filamentous haemagglutinin suggest a new model for two-partner secretion. Mol Microbiol. 2006; 62:641–654. [PubMed: 16999837]

Mazar J, Cotter PA. New insight into the molecular mechanisms of two-partner secretion. Trends Microbiol. 2007; 15:508–515. [PubMed: 17988872]

Menestrina G, Moser C, Pellet S, Welch R. Pore-formation by *Escherichia coli* hemolysin (HlyA) and other members of the RTX toxins family. Toxicology. 1994; 87:249–267. [PubMed: 8160187]

Mishra M, Parise G, Jackson KD, Wozniak DJ, Deora R. The BvgAS signal transduction system regulates biofilm development in *Bordetella* . J Bacteriol. 2005; 187:1474–1484. [PubMed: 15687212]

Mouallem M, Farfel Z, Hanski E. *Bordetella pertussis* adenylate cyclase toxin: intoxication of host cells by bacterial invasion. Infect Immun. 1990; 58:3759–3764. [PubMed: 2172167]

Nelson JD. The changing epidemiology of pertussis in young infants. The role of adults as reservoirs of infection. Am J Dis Child. 1978; 132:371–373. [PubMed: 645653]

Noel CR, Mazar J, Melvin JA, Sexton JA, Cotter PA. The prodomain of the *Bordetella* two-partner secretion pathway protein FhaB remains intracellular yet affects the conformation of the mature C-terminal domain. Mol Microbiol. 2012; 86:988–1006. [PubMed: 23035892]

Osicka R, Osickova A, Hasan S, Bumba L, Cerny J, Sebo P. *Bordetella* adenylate cyclase toxin is a unique ligand of the integrin complement receptor 3. eLife. 2015; 4

Osickova A, Masin J, Fayolle C, Krusek J, Basler M, Pospisilova E, et al. Adenylate cyclase toxin translocates across target cell membrane without forming a pore. Mol Microbiol. 2010; 75:1550–1562. [PubMed: 20199594]

O'Toole GA. Microtiter Dish Biofilm Formation Assay. J Vis Exp. 2011; 47:2437.

Park J, Zhang Y, Buboltz AM, Zhang X, Schuster SC, Ahuja U, et al. Comparative genomics of the classical *Bordetella* subspecies: the evolution and exchange of virulence-associated diversity amongst closely related pathogens. BMC Genomics. 2012; 13 545-2164-13-545.

Pearson RD, Symes P, Conboy M, Weiss AA, Hewlett EL. Inhibition of monocyte oxidative responses by *Bordetella pertussis* adenylate cyclase toxin. J Immunol. 1987; 139:2749–2754. [PubMed: 2888823]

Perez Vidakovics ML, Lamberti Y, van der Pol WL, Yantorno O, Rodriguez ME. Adenylate cyclase influences filamentous haemagglutinin-mediated attachment of *Bordetella pertussis* to epithelial alveolar cells. FEMS Immunol Med Microbiol. 2006; 48:140–147. [PubMed: 16965362]

Perkins DJ, Gray MC, Hewlett EL, Vogel SN. *Bordetella pertussis* adenylate cyclase toxin (ACT) induces cyclooxygenase-2 (COX-2) in murine macrophages and is facilitated by ACT interaction with CD11b/CD18 (Mac-1). Mol Microbiol. 2007; 66:1003–1015. [PubMed: 17927697]

Quinn HE, McIntyre PB. The impact of adolescent pertussis immunization, 2004–2009: lessons from Australia. Bull World Health Organ. 2011; 89:666–674. [PubMed: 21897487]

Sadilkova L, Osicka R, Sulc M, Linhartova I, Novak P, Sebo P. Single-step affinity purification of recombinant proteins using a self-excising module from *Neisseria meningitidis* FrpC. Protein Sci. 2008; 17:1834–1843. [PubMed: 18662906]

Sakamoto H, Bellalou J, Sebo P, Ladant D. *Bordetella pertussis* adenylate cyclase toxin. Structural and functional independence of the catalytic and hemolytic activities. J Biol Chem. 1992; 267:13598–13602. [PubMed: 1618862]

Sebo P, Ladant D. Repeat sequences in the *Bordetella pertussis* adenylate cyclase toxin can be recognized as alternative carboxy-proximal secretion signals by the Escherichia coli alpha-haemolysin translocator. Mol Microbiol. 1993; 9:999–1009. [PubMed: 7934926]

Serra D, Bosch A, Russo DM, Rodriguez ME, Zorreguieta A, Schmitt J, et al. Continuous nondestructive monitoring of *Bordetella pertussis* biofilms by Fourier transform infrared spectroscopy and other corroborative techniques. Anal Bioanal Chem. 2007; 387:1759–1767. [PubMed: 17216159]

Serra DO, Conover MS, Arnal L, Sloan GP, Rodriguez ME, Yantorno OM, Deora R. FHA-mediated cell-substrate and cell-cell adhesions are critical for *Bordetella pertussis* biofilm formation on abiotic surfaces and in the mouse nose and the trachea. PLoS One. 2011; 6:e28811. [PubMed: 22216115]

Sisti F, Ha DG, O'Toole GA, Hozbor D, Fernandez J. Cyclic-di-GMP signalling regulates motility and biofilm formation in *Bordetella bronchiseptica* . Microbiology. 2013; 159:869–879. [PubMed: 23475948]

Sloan GP, Love CF, Sukumar N, Mishra M, Deora R. The *Bordetella* Bps polysaccharide is critical for biofilm development in the mouse respiratory tract. J Bacteriol. 2007; 189:8270–8276. [PubMed: 17586629]

Sorroche FG, Spesia MB, Zorreguieta A, Giordano W. A positive correlation between bacterial autoaggregation and biofilm formation in native Sinorhizobium meliloti isolates from Argentina. Appl Environ Microbiol. 2012; 78:4092–4101. [PubMed: 22492433]

Strebel P, Nordin J, Edwards K, Hunt J, Besser J, Burns S, et al. Population-based incidence of pertussis among adolescents and adults, Minnesota, 1995–1996. J Infect Dis. 2001; 183:1353–1359. [PubMed: 11294666]

Sugisaki K, Hanawa T, Yonezawa H, Osaki T, Fukutomi T, Kawakami H, et al. Role of (p)ppGpp in biofilm formation and expression of filamentous structures in *Bordetella pertussis*. Microbiology. 2013; 159:1379–1389. [PubMed: 23676431]

Thorstensson R, Trollfors B, Al-Tawil N, Jahnmatz M, Bergstrom J, Ljungman M, et al. A phase I clinical study of a live attenuated *Bordetella pertussis* vaccine--BPZE1; a single centre, double-blind, placebo-controlled, dose-escalating study of BPZE1 given intranasally to healthy adult male volunteers. PLoS One. 2014; 9:e83449. [PubMed: 24421886]

Uribe KB, Martin C, Etxebarria A, Gonzalez-Bullon D, Gomez-Bilbao G, Ostolaza H. Ca2+ influx and tyrosine kinases trigger *Bordetella* adenylate cyclase toxin (ACT) endocytosis. Cell physiology and expression of the CD11b/CD18 integrin major determinants of the entry route. PLoS One. 2013; 8:e74248. [PubMed: 24058533]

Vergara-Irigaray N, Chavarri-Martinez A, Rodriguez-Cuesta J, Miller JF, Cotter PA, Martinez de Tejada G. Evaluation of the role of the Bvg intermediate phase in *Bordetella pertussis* during experimental respiratory infection. Infect Immun. 2005; 73:748–760. [PubMed: 15664913]

Vojtova J, Kofronova O, Sebo P, Benada O. *Bordetella* adenylate cyclase toxin induces a cascade of morphological changes of sheep erythrocytes and localizes into clusters in erythrocyte membranes. Microsc Res Tech. 2006; 69:119–129. [PubMed: 16456835]

Weiss AA, Hewlett EL, Myers GA, Falkow S. Tn5-induced mutations affecting virulence factors of *Bordetella pertussis*. Infect Immun. 1983; 42:33–41. [PubMed: 6311749]

Wendelboe AM, Njamkepo E, Bourillon A, Floret DD, Gaudelus J, Gerber M, et al. Transmission of *Bordetella pertussis* to young infants. Pediatr Infect Dis J. 2007; 26:293–299. [PubMed: 17414390]

Zaretzky FR, Gray MC, Hewlett EL. Mechanism of association of adenylate cyclase toxin with the surface of *Bordetella pertussis*: a role for toxin-filamentous haemagglutinin interaction. Mol Microbiol. 2002; 45:1589–1598. [PubMed: 12354227]

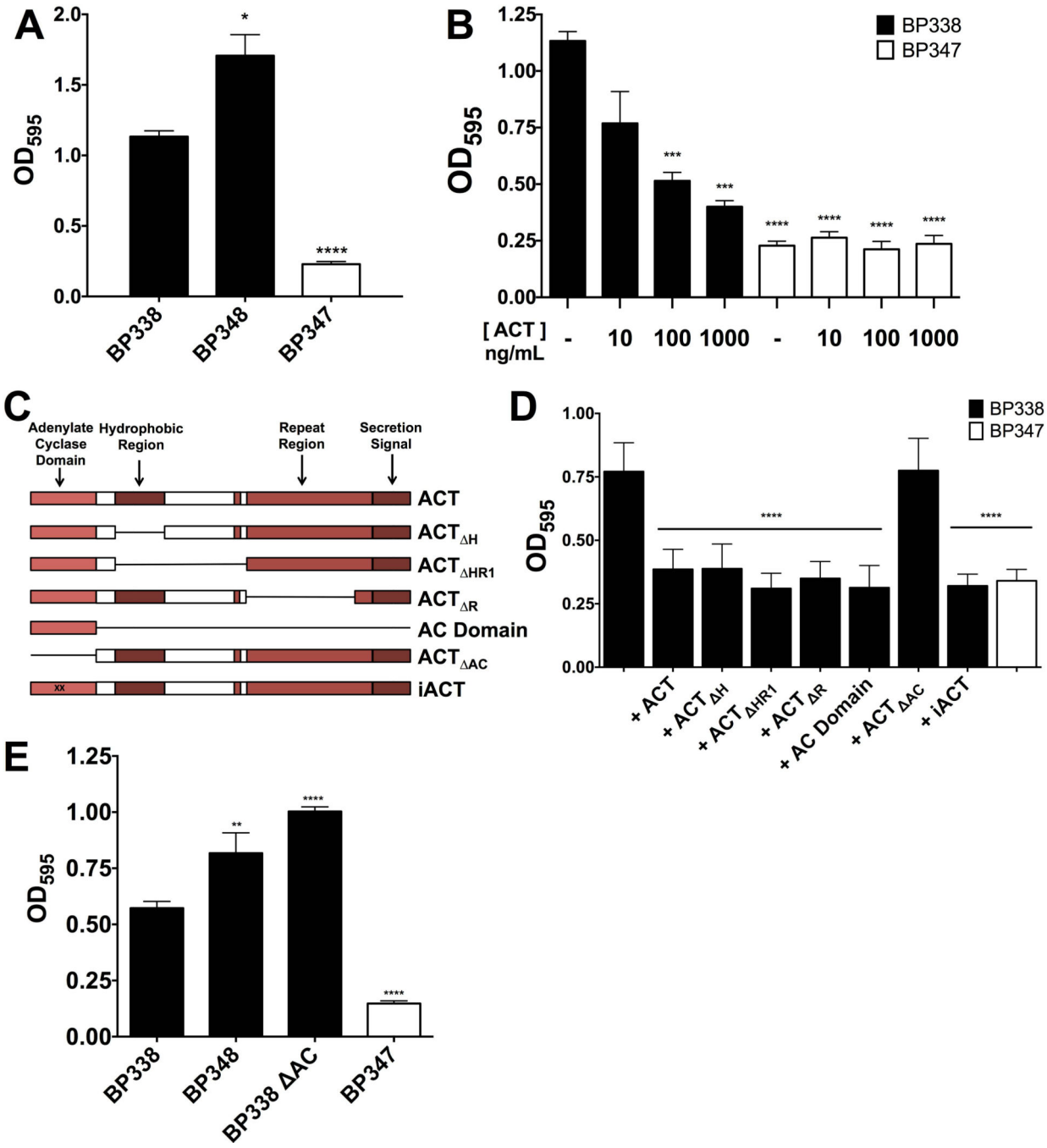

Figure 1.

(A) BP348, a *B. pertussis* strain lacking ACT, makes more biofilm than WT BP338 *B. pertussis*. Strains were grown in 96 well microtiter plates and biofilm formation was assessed using the crystal violet assay at 96 hours. Bvg(−) BP347 serves as a negative control. Data expressed as the mean ± standard deviations, compiled from 3 experiments run in triplicate. * = $p < 0.05$ and **** = $p < 0.0001$ compared to WT BP338. **(B) ACT inhibits biofilm in a concentration-dependent manner**. WT BP338 biofilm formation in the presence of increasing concentrations of recombinant purified ACT (ng mL^{-1}) was assessed

at 96 hours. Biofilm formation was measured by crystal violet assay. Bvg(−) BP347 serves as negative control. Data expressed as the mean ± standard deviations, compiled from 5 experiments run in triplicate. *** = p <0.001, **** = p <0.0001 compared to WT BP338 without ACT. **(C)** Schema of ACT truncated and enzymatically inactive mutant proteins (Lee *et al.*, 1999). **(D) The AC domain is necessary and sufficient for biofilm inhibition, although the catalytic activity of ACT is not required**. ACT, iACT or other ACT mutant proteins were added to WT BP338 and biofilm formation was measured by crystal violet assay at 96 hours. AC domain was added at 10 ng mL^{-1} and additional ACT proteins including ΔH, ΔHR1, ΔR, and ΔAC were all added to a final concentration of 100 ng mL^{-1}. Data expressed as the mean ± standard deviations, compiled from 3 experiments run in triplicate. *** = p <0.0005 compared to WT BP338 without ACT. **(E) BP338 lacking the AC domain (BP338 ΔAC) makes more biofilm than the parental WT strain**. Strains were grown in 96 well microtiter plates and biofilm formation was assessed using the crystal violet assay at 96 hours. Mean values represented by bars, error bars represent standard deviations. Bvg(−) strain serves as a negative control. Data expressed as the mean ± standard deviations, compiled from 3 experiments run in triplicate. ** = p <0.01 and **** = p <0.0001 compared to WT.

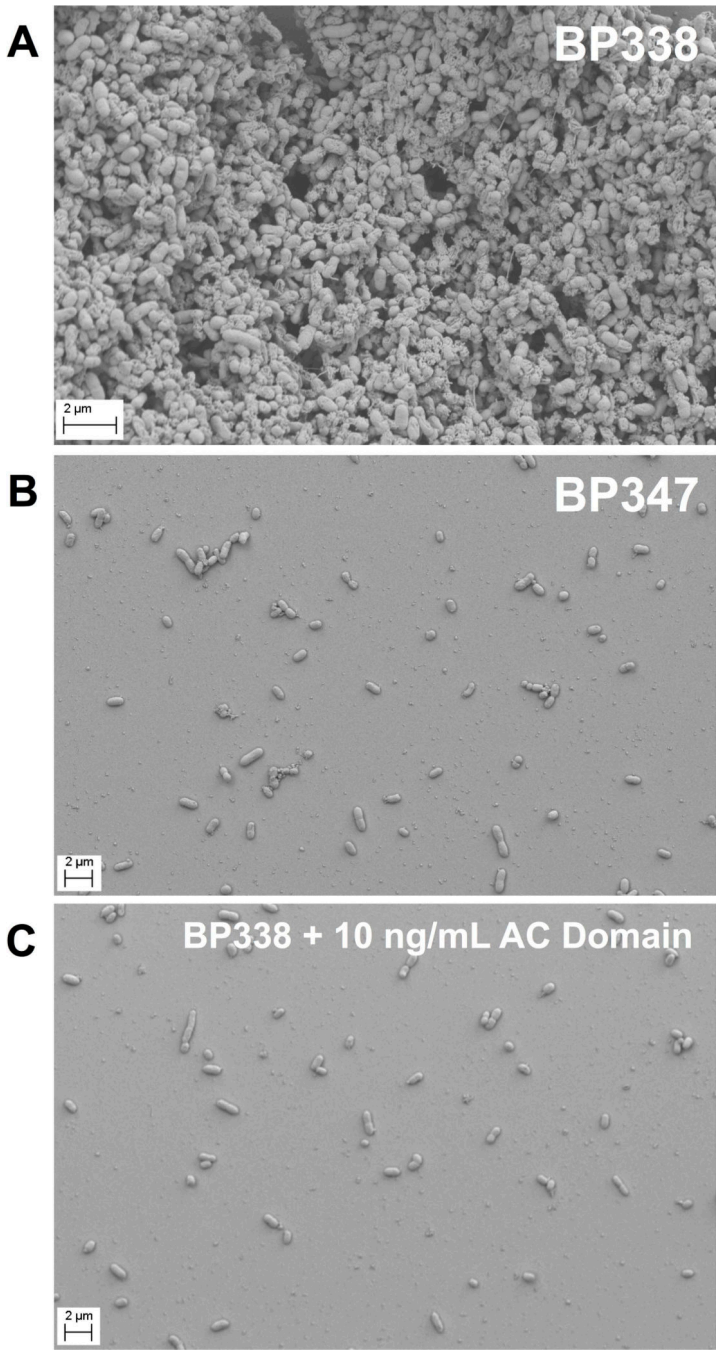

Figure 2. SEM images show that AC domain inhibits biofilm formation on glass coverslips

B. pertussis was grown in 24 well plates with inverted glass coverslips so that biofilm formation could occur at the air liquid interface. At 96 hours, the coverslips were fixed in 4% paraformaldehyde and prepared for SEM imaging using a Zeiss Sigma VP HD field emission Scanning Electron Microscope at the University of Virginia Microscopy Core. Representative images were chosen from four experimental replicates. **(A)** WT BP338 (15000 X). **(B)** Bvg(−) BP347 *B. pertussis* (5000 X). **(C)** WT BP338 + 10 ng mL^{-1} AC domain (5000 X).

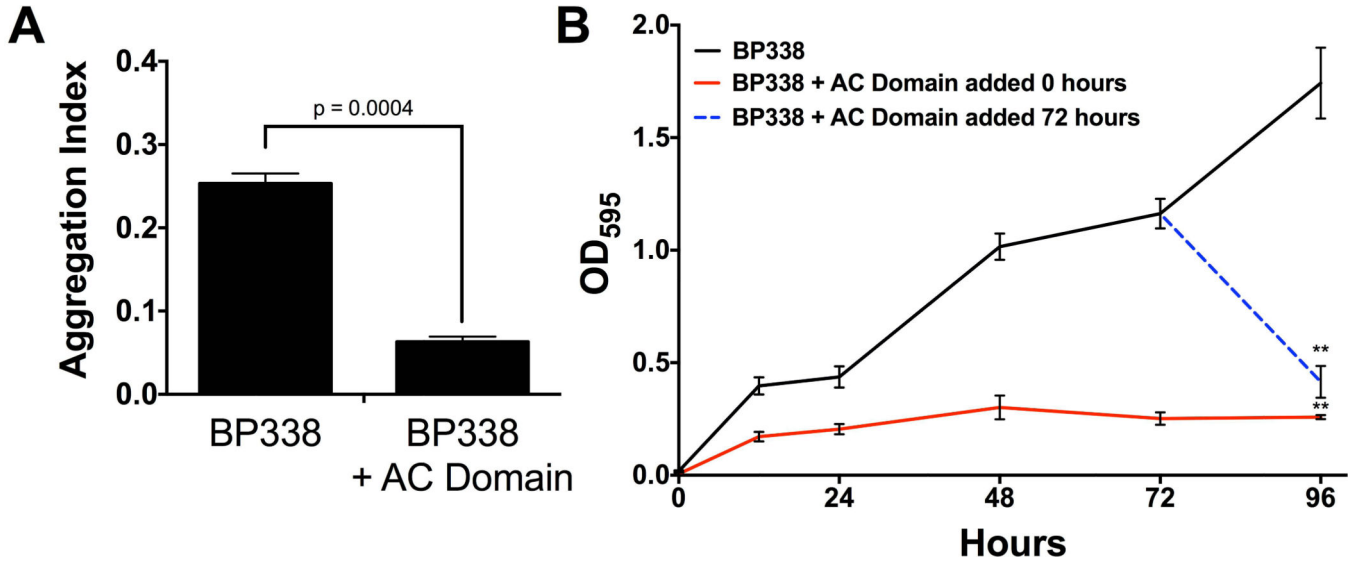

Figure 3.

(A) Exogenous AC domain inhibits bacterial aggregation. *B. pertussis* strains were grown as 5 mL shaking cultures, in the presence or absence of 100 ng/mL AC domain. At 24 hours, samples were removed from the culture and the Aggregation Index was determined. Mean values are represented by bars, error bars represent standard deviations. Data expressed as the mean ± standard deviations, compiled from 3 experiments run in triplicate. **(B) Exogenous AC domain disrupts preformed biofilm**. BP338 biofilm formation (circles, black line) was measured every 24 hours via the crystal violet assay. AC domain was added at time zero (squares, red line) or was added at 72 hours (open blue circles, dashed line) and biofilm was measured every 24 hours. Mean values represented by lines and error bars represent standard deviations. Data compiled from 5 experiments run in triplicate. ** = $p < 0.001$ compared to BP338.

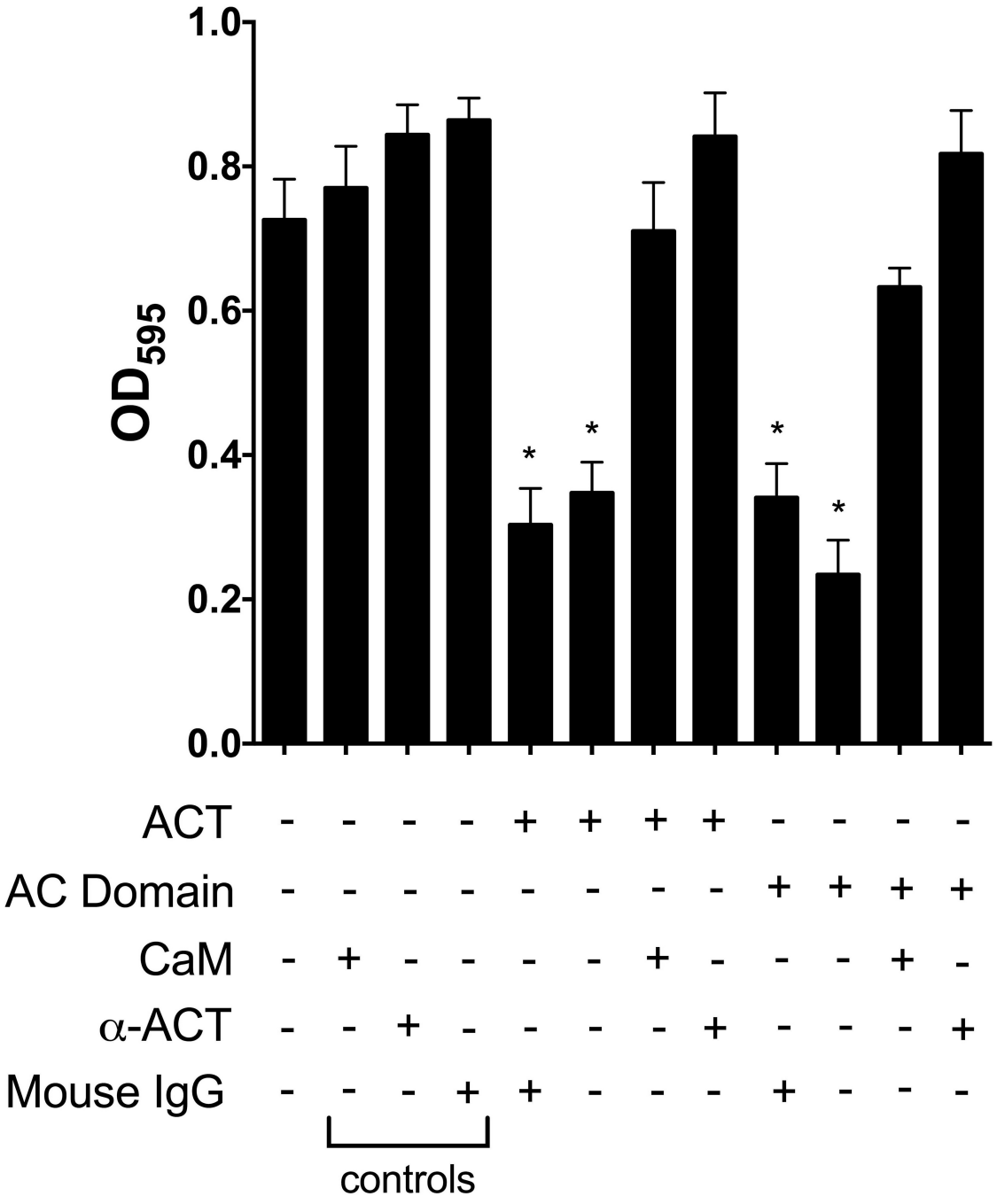

Figure 4. CaM and anti-ACT antibodies block ACT inhibitory effects

Calmodulin (1 μM) was incubated with ACT (100 ng mL^{-1}, 565 pM) or AC domain (10 ng mL^{-1}, 0.233 pM) for 15 minutes before adding the combination to BP338 cultures. ACT and AC domain alone were also incubated for 15 minutes prior to addition to bacterial cultures. Monoclonal antibody 7CE4B1 directed against the AC domain (Lee *et al.*, 1999), produced by Hewlett Lab, (2.4 μg mL^{-1}) was incubated with ACT or AC domain for 15 minutes before adding the combination to cultures in 96 well microtiter plates. Mixtures as indicated were added to bacterial cultures and biofilm formation was measured at 96 hours by crystal

violet assay. Data expressed as the mean ± standard deviations, compiled from 3 experiments run in triplicate. * = $p < 0.05$ compared to WT.

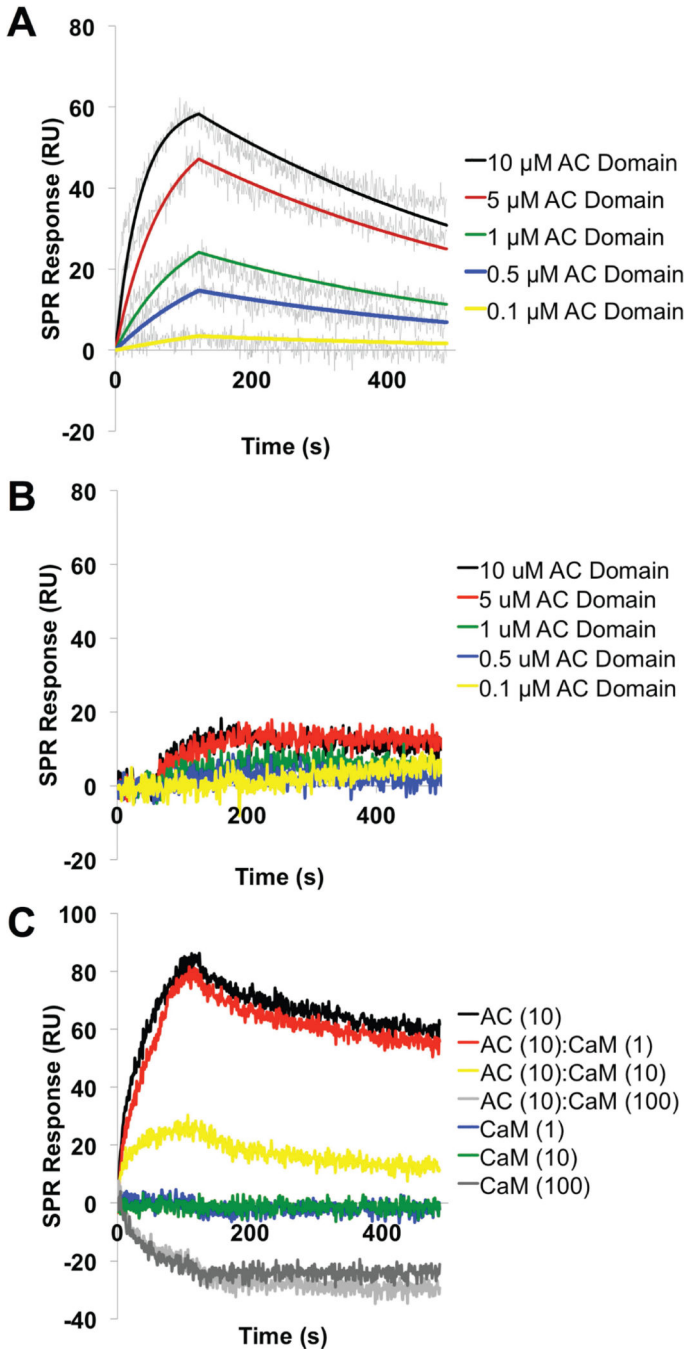

Figure 5. SPR kinetic binding analysis of the interaction between FHA and the AC domain of ACT

The recombinant AC domain at indicated concentrations was injected in parallel ("one-shot kinetics") over the sensor chip coated with purified **(A) FHA** or **(B) FHA44** proteins at a flow rate of 30 μL/min for both association and dissociation phases of the sensogram. The kinetic data were fitted globally by using a 1:1 Langmuir model (see Materials and Methods) to obtain association [k_a=2.9±0.4 (×10^3) $M^{-1}s^{-1}$] and dissociation [k_d=1.9±0.2 (×10^{-2}) s^{-1}] rate constants of the interaction. The equilibrium dissociation constant, K_D, was determined as k_d/k_a and found to be 650 nM between AC domain and FHA. No binding was observed

between AC domain and FHA44. The fitted curves are superimposed as colored lines on top of the binding curves. Representative data from a single experiment shown here. **(C) CaM blocks the AC domain – FHA interaction**. The AC domain (10 μM) and the freshly-prepared complexes of the AC domain with CaM mixed in molar ratios of 10:1, 1:1 and 1:10 AC domain:CaM were injected in parallel over the SPR sensor chip coated with FHA at flow rate of 30 μL/min. Inhibition of binding of the AC/CaM 1:10 complex to FHA is represented by a decrease of SPR signal response. No binding of CaM alone was observed to FHA. Results are representative data from three independent experiments.

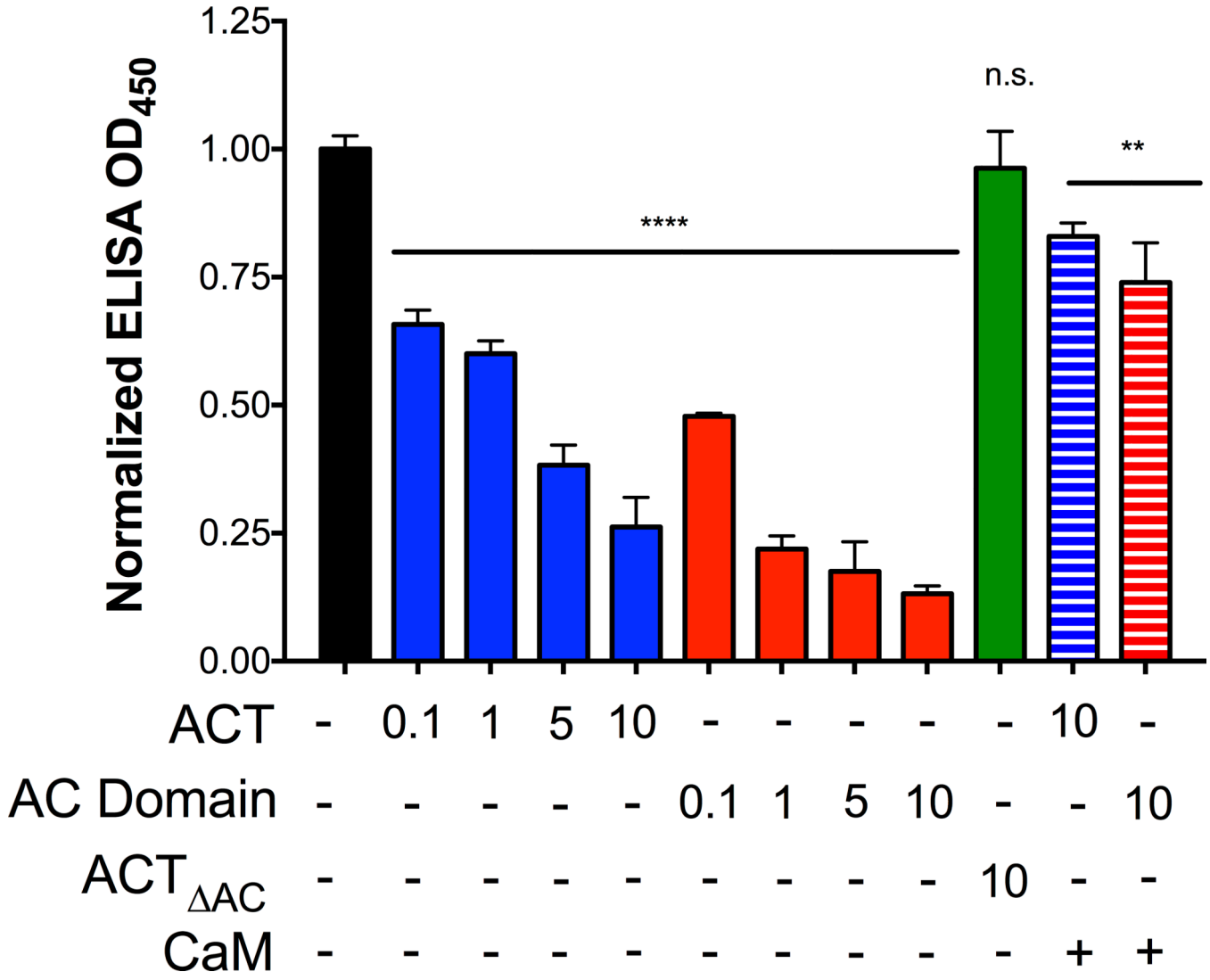

Figure 6. The AC domain and ACT inhibit MCD antibody binding to FHA

In an ELISA binding assay, plates were coated with FHA and an anti-MCD antibody was used as a detection reagent. ACT, AC domain and $ACT_{\Delta AC}$, added at a range of μg mL^{-1} concentrations, were added prior to the addition of the anti-MCD antibody to determine if AC domain binding interfered with MCD antibody detection. In addition to these conditions, 10 μM CaM was incubated with the various concentrations of ACT or AC domain for 15 minutes prior to addition of ACT to the wells. All values were normalized to the control (OD_{450} 0.284) using GraphPad Prism6 software. Data expressed as the mean ± standard deviations, compiled from 3 experiments run in triplicate ** = p <0.01 and **** = p<0.0001 compared to control.

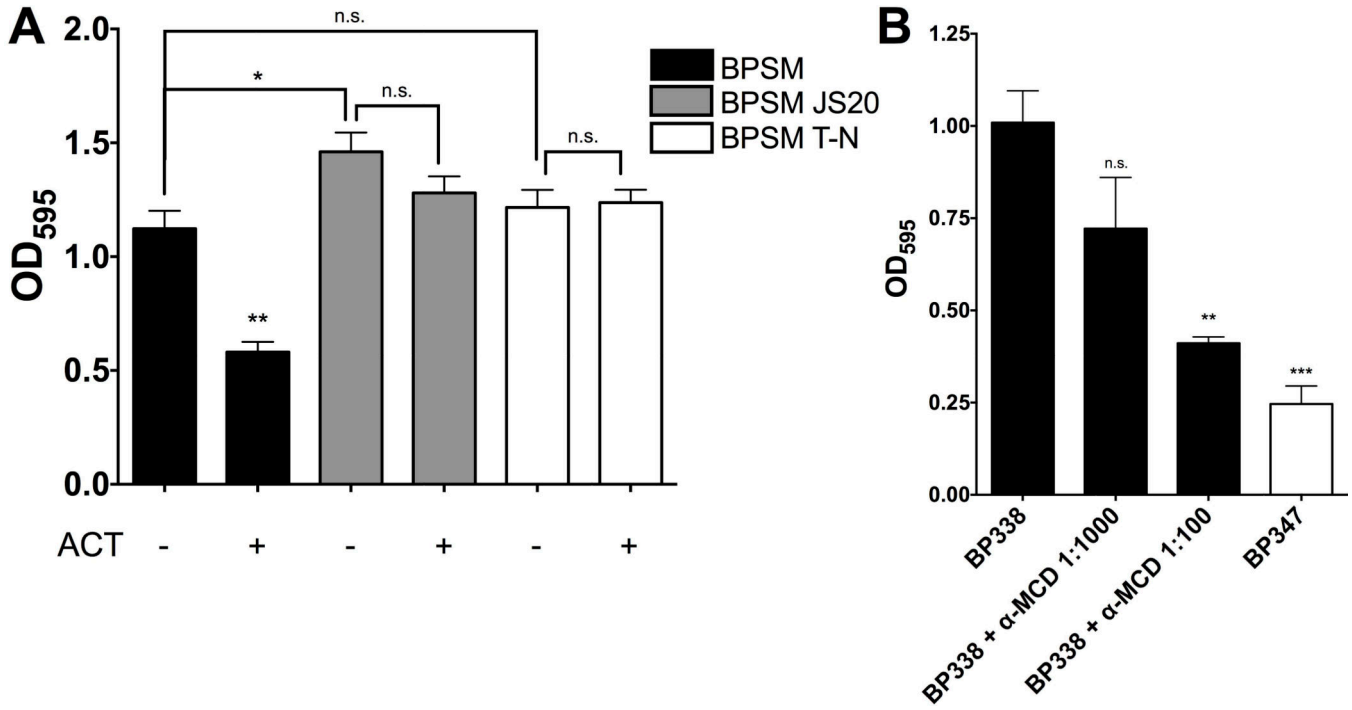

Figure 7.

(A) The MCD of FHA must be present and properly folded for ACT inhibition of biofilm. FHA mutant proteins were generated in the WT *B. pertussis* BPSM parent strain. BPSM JS20 (ΔMCD) has the entire MCD sequence deleted. BPSM T-N has a transposon inserted into the prodomain sequence, precluding prodomain cleavage and processing of the MCD, leaving the MCD unfolded in the final FHA molecule. *B. pertussis* strains were allowed to form biofilm for 96 hours in the presence or absence of 100 ng mL^{-1} ACT. Biofilm was measured by crystal violet assay. Data expressed as the mean ± standard deviations, compiled from 3 experiments run in triplicate. * = $p < 0.05$ and ** = $p < 0.01$ compared to WT (BPSM). **(B) Anti-MCD antibodies block biofilm**. Anti-MCD antibodies were added at 1:1000 and 1:100 dilutions to WT *B. pertussis* (BP338) cultures in 96 well microtiter plates to observe their effects on biofilm formation. Biofilm formation was measured at 96 hours using the crystal violet assay. All values were normalized to the control (OD450 0.284) using Graphpad Prism6 software. Data expressed as the mean ± standard deviations, compiled from 3 experiments run in triplicate ** = $p < 0.01$ compared to WT alone.

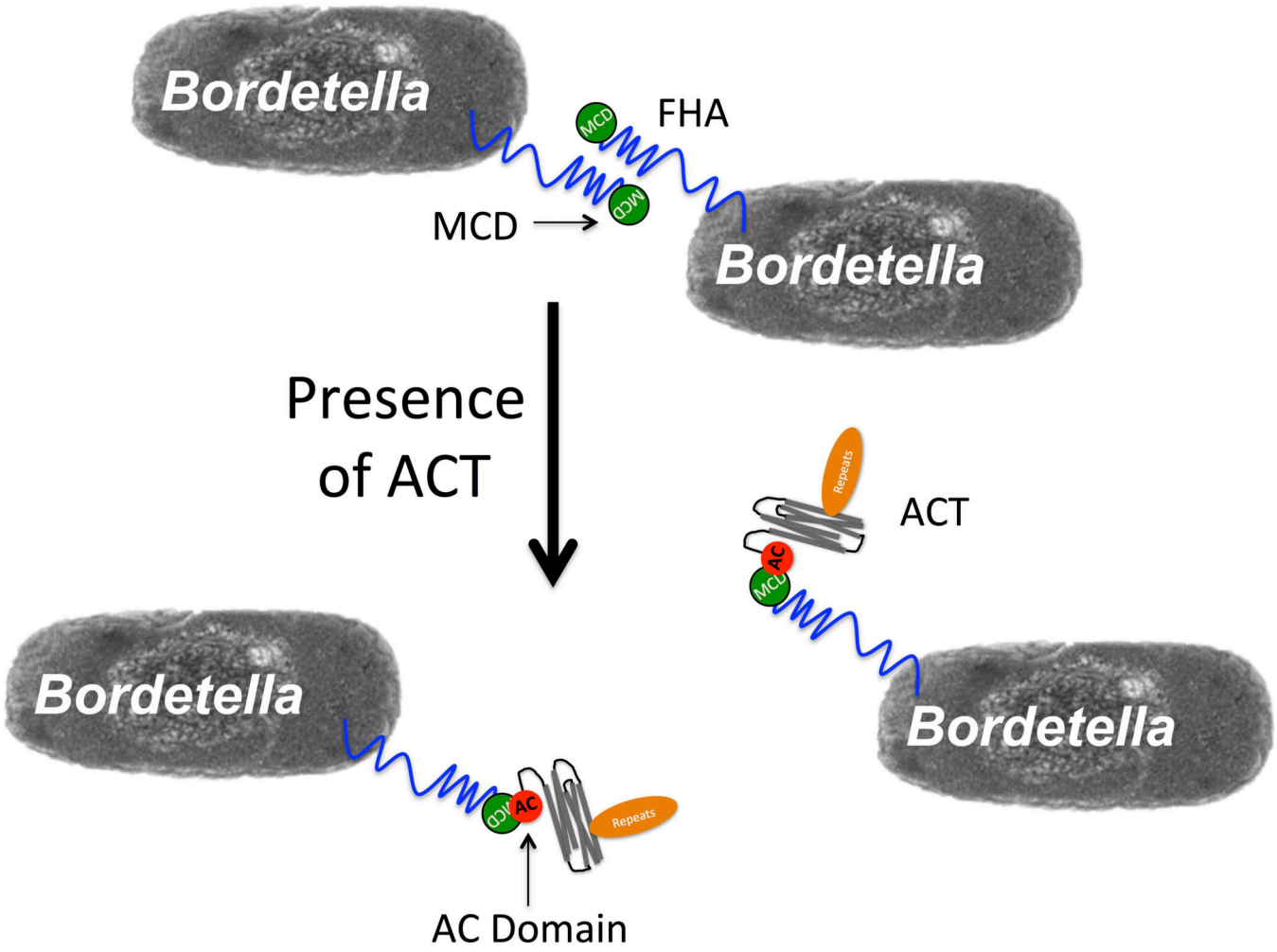

Figure 8. Working model of biofilm inhibition by ACT

The AC domain of ACT binds FHA via the MCD at the distal tip of the FHA molecule. This binding blocks FHA function in biofilm, either through FHA-FHA interactions within biofilm or FHA-surface interactions as previously suggested, or possibly through some signaling event due to conformation change in the FHA protein.